TOUGHENING MECHANISMS IN PLAIN AND FIBER REINFORCED CONCRETE

Victor C. Li
Department of Civil Engineering, Massachusetts Institute of Technology
Cambridge, MA 02139, USA

ABSTRACT

The fracture toughness of plain concrete and fiber reinforced concrete relies on the presence of weak interfaces within the material structure. This paper reviews the role of the internal material structures in controlling the fracture toughness in these materials. Special emphasis is placed on the relation between the deformation mechanisms associated with the material structure and the macroscopic tension-softening behavior.

INTRODUCTION

When a brittle material is subjected to tensile stresses beyond the linear elastic range, some form of inelastic internal deformation mechanism, distributed over the material volume occurs. In cement, this may be microcracking at defect sites such as that associated with air voids. In concrete, the internal inelastic deformation may be associated with the nucleation and subsequent enlargement of mortar/aggregate interfacial cracks. In fiber reinforced concrete, mortar matrix cracking, fiber debonding and pull-out or rupture may follow elastic deformation. All of these internal deformation mechanisms contribute to macroscopic non-linear stress-strain behavior. Further loading may lead to localization of inelastic deformation on a macroscopically single fracture plane, as is observed in cement, concrete and in certain fiber reinforced cementious composites (FRC). The formation of this fracture plane signifies a limit on the maximum tensile load bearing capacity of the material. However, the tensile traction acting across this plane does not necessarily drop to zero immediately, but usually decreases as a function of the amount of separation of the opposite faces of this plane. The functional relationship between this traction σ and the fracture surface separation δ is generally termed the tension-softening curve or σ–δ curve of a given material. For example, Figure 1 shows typical σ–δ curves for mortar, concrete and synthetic FRC. Clearly, the shape of the tension-softening curve is closely related to the internal deformation mechanisms of the material. The internal deformation mechanisms must in turn be closely related to the internal material structure.

It has been shown [1] that the area under the σ–δ curve is equal to the critical energy release rate (directly related to the fracture toughness) of a material. From Figure 1, it can be inferred that the toughness increases from mortar to concrete to FRC. Figure 2 shows the typical range of toughness for cement [2], concrete [3] and acrylic fiber reinforced concrete [4]. Apart from toughness, the σ–δ curve has also been related to the macroscopic behavior of a structure [e.g. 5, 6] and with R-curve behavior [e.g.7].

MRS Int'l. Mtg. on Adv. Mats. Vol. 5

In this paper we review recent theoretical and experimental work on the relationship between material internal structure and the tension-softening curve for concrete and synthetic FRC, with a view toward the deployment of such knowledge to engineering toughness in these materials. The discussion on concrete has stronger emphasis on theoretical modelling, whereas the discussion on FRC has a stronger emphasis on experimental observations. The research work reviewed are based on that conducted at the Center for Advanced Construction Materials at MIT, and are not meant to be a comprehensive coverage of increasing amount of activities in this field of research.

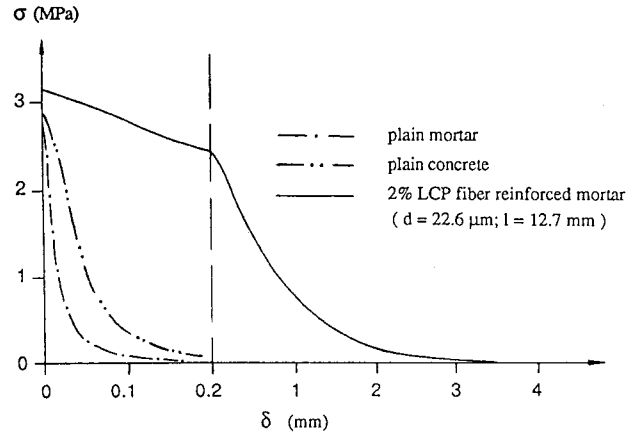

Figure 1. Typical Tension-Softening Curves for Mortar, Concrete and Synthetic FRC

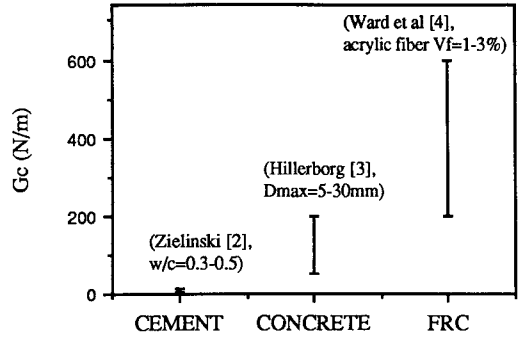

Figure 2. Fracture Toughness Range of Cement, Concrete and Synthetic FRC

A hallmark of our current approach is to focus attention on modelling and experimental determination of the uniaxial tension-softening relationship of a material, assuming that such a relationship can predict (analytically or numerically) R-curve behavior of any given specimen

geometry and loading condition. This is in contrast to many published work on directly modeling or measuring R-curve behavior, which involves complex interactions between an assumed pre-existing macrocrack and the internal deformation mechanisms at the crack tip zone.

INTERNAL STRUCTURE, TOUGHENING MECHANISMS AND POST-PEAK BEHAVIOR OF PLAIN CONCRETE

The internal structure of concrete is made up of mainly cement paste (including air voids) and aggregates. Figure 3 (after Wittmann [8]) shows the simulated structure of concrete with (a) aggregates having random geometry and with (b) aggregate size distribution following the Fuller curve. Between the cement paste and aggregates are interfacial zones which often form the material weak link. Interfacial defects may be due to cement shrinkage stresses during curing [9] and/or due to bleeding [10].

The growth of a single interfacial crack under ambient tensile load at a cement/aggregate interface has been analyzed by Cherepanov and reported by Zaitsev [11]. The result is plotted in Figure 4 relating the equilibrium load to the angular crack dimension, θ. A family of four curves are shown for different aggregate radii R to illustrate the fact that for any given ambient load σ*, aggregates with radii from R_{crit} to R_{max} could have interfacial cracks larger than $\theta_1 \approx \pi/4$, where R_{max} is the largest aggregate size. For initial flaw sizes less than θ_1, flaw size expansion is unstable and may be considered as spontaneous nucleation of interfacial cracks. Further stable expansion after θ_1 requires increasing load. However at θ_2 branching of the interfacial crack into the matrix will occur. The exact value of θ_2 depends on the ratio of interfacial to cement matrix toughness K_{Ic}^{if}/K_{Ic}^{m}. For normal concrete, this ratio is typically around 0.6 and $\theta_2 \approx \pi/2$. Growth of branch crack corresponding to the negative sloped line beyond $\theta = \theta_2$ initiates at the largest aggregate.

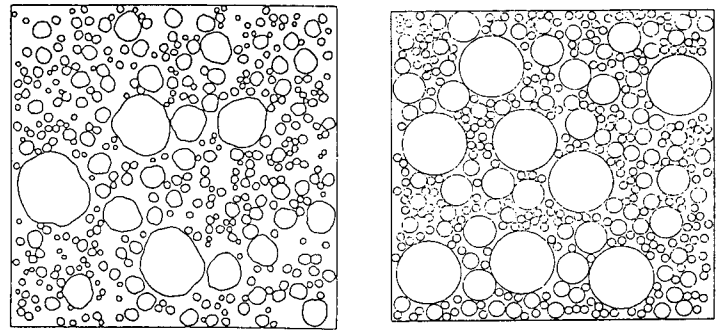

Figure 3. Simulated Internal Structure of Concrete [8] with (a) Aggregates Having Random Geometry and (b) Aggregate Size Distribution Following the Fuller Curve

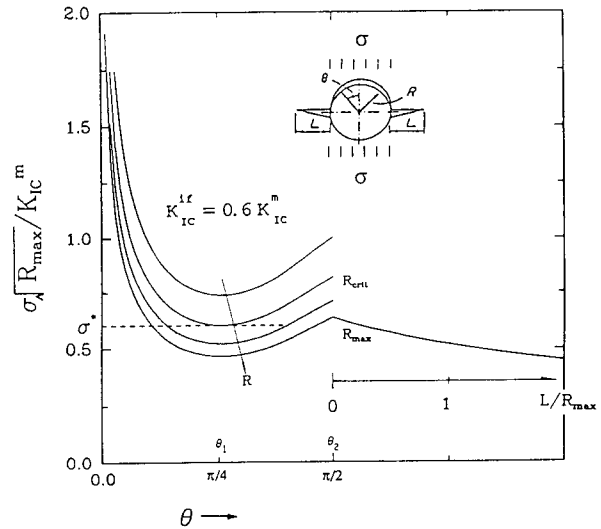

Figure 4. Equilibrium Load as a Function of Dimension of Interfacial and Branch Cracks [11]

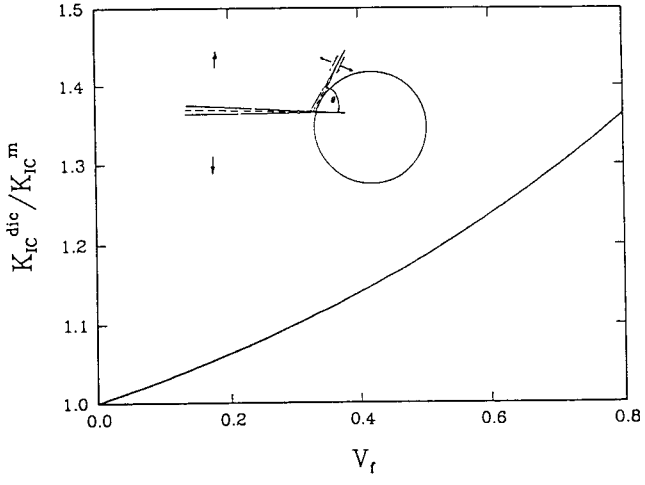

Figure 5. Crack Tip Deflection Toughening

The post-peak tension-softening behavior of concrete was modelled by Li and Huang [12], and Huang and Li [13]. They associated the peak tensile strength with the first branching of an interfacial crack into the cement matrix. Subsequent tension-softening was modelled by the

expansion of this dominant crack as one which encounters an effectively homogeneous material. This homogeneous material will have a toughness higher than the cement matrix toughness K_{Ic}^{m}. Two toughening mechanisms were accounted for: Crack tip deflection toughening, shown schematically in the insert of Figure 5, assumes that the dominant crack tip is deflected whenever it intersects an aggregate. The amount of toughening K_{Ic}^{def}/K_{Ic}^{m}, where K_{Ic}^{def} is the effective toughness when crack tip deflection is considered, depends on the volume fraction of aggregates V_f and is shown in Figure 5. In a truly three dimensional system, the dominant crack front may deflect as well as twist around the aggregates. This toughening effect may be accounted for using the technique of Faber et al. [14]. Distributed interfacial crack toughening assumes that the dominant crack tip experiences a cloud of interfacial cracks, shown schematically in the insert of Figure 6, which effectively reduces the Young's modulus of the material in the crack tip zone. Calculation of the amount of toughening K_{Ic}^{dic}/K_{Ic}^{m}, where K_{Ic}^{dic} is the effective toughness when distributed interfacial cracks are considered, again lead to an expression dependent on V_f, if each aggregate is associated with one interfacial crack. This is illustrated in Figure 6. The amount of toughening, dependent on the Young's modulus contrast inside and outside of the process zone, may be overestimated because interfacial cracks should exist outside the crack tip zone prior to fracture localization, thus reducing the Young's modulus contrast. On the other hand, it may be expected that the high stress field ahead of the dominant crack tip will lead to enhanced branching of interfacial cracks into the cement matrix at aggregate sites there, as is usually observed. This should argue for an enhanced Young's modulus contrast.

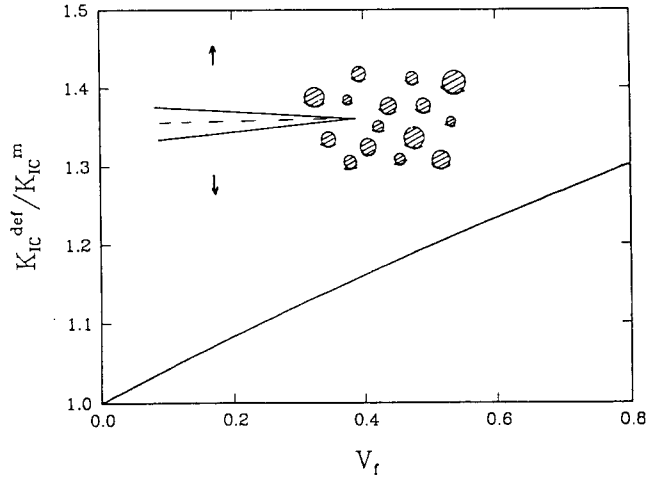

Figure 6. Distributed Interfacial Crack Toughening

The expansion of the dominant crack against the aggregate toughness of the matrix material leads to the tension-softening curve shown in Figure 7. The model parameters f_t, E and V_f have

been chosen to correspond to the concrete material tested by Reinhardt [15]. His experimental data are also shown in Figure 7.

The trade-off between the tensile strength and the fracture toughness of concrete predicted by the model is shown in Figure 8. The figure shows that the tensile strength drops with a simultaneous increase in the fracture toughness with larger maximum aggregate size. These calculations are done using a typical concrete mix design rule which relates V_f to D_{max} (= 2 R_{max}) in order to maintain concrete workability in the fresh state.

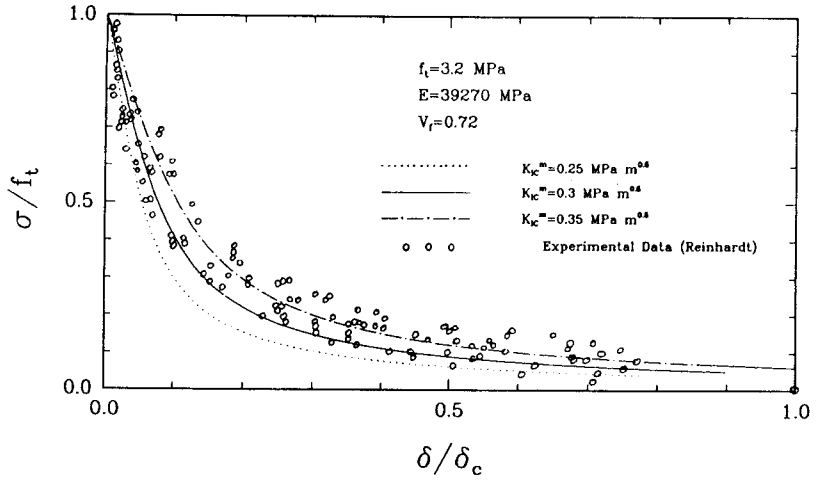

Figure 7. Predicted and Experimentally Deduced Tension-Softening Curve for Concrete

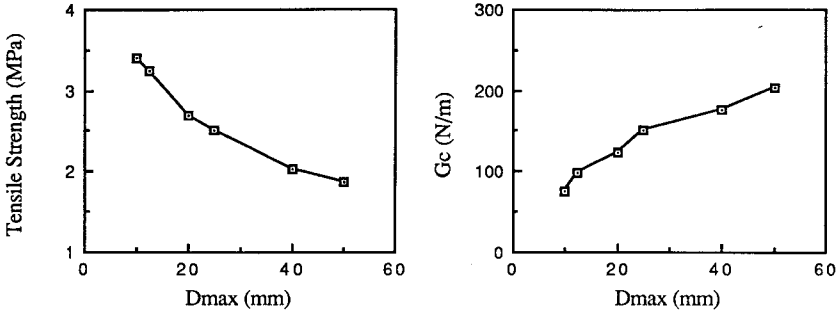

Figure 8. Predicted Trade-off between Tensile Strength and Fracture Toughness of Concrete with Increasing Aggregate Size D_{max} = 2 R_{max}

Comparison between model predicted G_c was made with concrete data collected by Hillerborg [3] and with recent data from Mihashi et al. [16] (they actually measured G_F), shown in Figure 9. The solid line is a linear regression for all the data points. For fixed D_{max}, the model predicts increasing G_c with V_f. Comparisons with data obtained by Shah and McGarry [17] (D_{max} fixed for the two mortars, D_{max} larger for concrete) from a series of tests with different specimen notch lengths are shown in Figure 10. These comparisons show that the tension-softening behavior and fracture toughness can be modelled in terms of the internal material structures and deformation mechanisms.

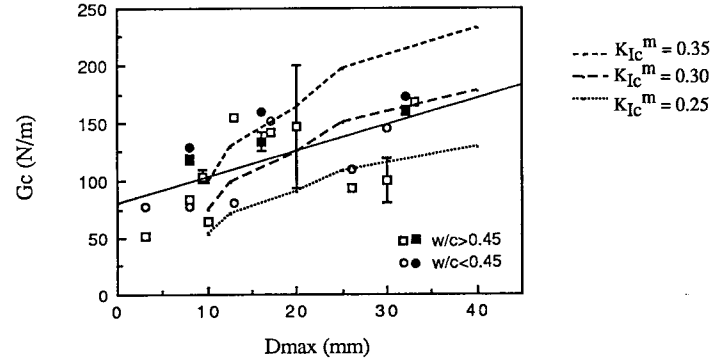

Figure 9. Predicted and Experimentally Determined Concrete Fracture Toughness Increase with Maximum Aggregate Size. Open Symbols are Data Collected by Hillerborg [3], Closed Symbols are Data from Mihashi et al [16].

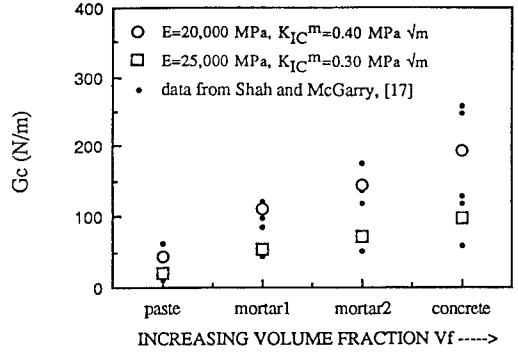

Figure 10. Predicted and Experimentally Determined Concrete Fracture Toughness Increase with Aggregate Volume Fraction

The following conclusions may be drawn: Both experimental data and model predictions show that post-peak behavior of concrete is controlled by R_{max}, V_f, K_{Ic}^{m} and K_{Ic}^{if}. Specifically the fracture toughness increases with V_f and R_{max}. Similar conclusions based on experimental tests of cementitious materials [17, 18] and other particulate composites [19] have been reached by other researchers. This implies that more weak interfaces are good for toughness. However this is gained at the expense of tensile strength, at least for conventional concrete mix designs. Some methods of high strength concrete production involving the increase of cement/aggregate bond strength or using very small aggregate sizes, may mean the reduction of weak interfaces, leading to material brittleness. In essence, the toughening mechanisms of crack deflection and distributed interfacial cracking would be significantly hindered. Finally the model suggests that a high cement matrix toughness may lead to increase in both tensile strength and fracture toughness.

INTERNAL STRUCTURE, TOUGHENING MECHANISMS AND POST-PEAK BEHAVIOR OF SYNTHETIC FIBER REINFORCED CONCRETE

In synthetic fiber reinforced concrete, the ultimate (or critical) strain of the concrete matrix is usually much smaller than that of the fibers. Thus matrix cracking results in a fracture plane bridged by fibers, usually in the form of bundles, at random orientation with respect to the fracture plane. For example, Figure 11 shows an SEM graph of a fracture plane of an acrylic fiber reinforced mortar.

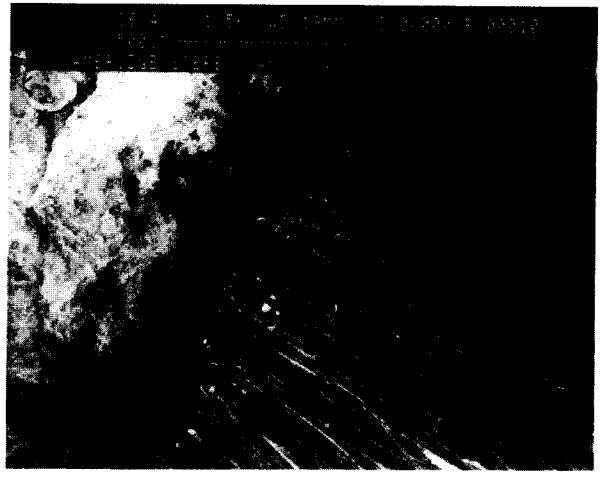

Figure 11. SEM graph of a FRC Fracture Surface Showing a Bundle of Acrylic Fibers

The presence of fibers leads to a dramatic change in the post-peak behavior of the mortar, as illustrated in Figure 12, which shows the load versus crack face separation curve from a stable direct tension test of a liquid crystal polyester (LCP) fiber reinforced mortar. A structural component may have quite drastic increases in ductility due to fiber reinforcement, and is illustrated by the flexural curves from 3-point bend tests [20] of several FRC beams in Figure 13. Enhancement of fracture toughness usually increases with fiber volume fraction, as long as the workability of the material is adequately maintained. Figure 14 shows a 600% increase in fracture toughness for a 3% V_f acrylic fiber reinforced mortar over plain mortar, based on two test methods [4].

To understand the physical mechanisms of toughening in synthetic FRC, studies of mono-filament pull-out have been conducted [21]. These experimental studies reveal an interesting phenomenon. The pull-out curves for nylon and polypropylene (Figure 15) indicate that subsequent to end slippage (point A), the crack separation is accompanied by increasing load (rather than decreasing load) for some amount prior to load reduction associated with decreasing contact surface as the fiber slides out. Furthermore the load decreases to zero (point B) after crack separation larger than the embedded length of the short end. This behavior may be explained by a frictional bond which increases with sliding distance, rather than uniform as is usually assumed [21]. Observational evidence of fiber abrasion (Figure 16) appears to support this hypothesis.

Increased frictional bond due to fiber abrasion implies large amount of inelastic energy absorption during the fiber pull-out process accompanying the tension-softening behavior of the FRC composite. This is probably the dominant contributor to the enhanced fracture toughness of FRC even though other energy absorption mechanisms may operate simultaneously.

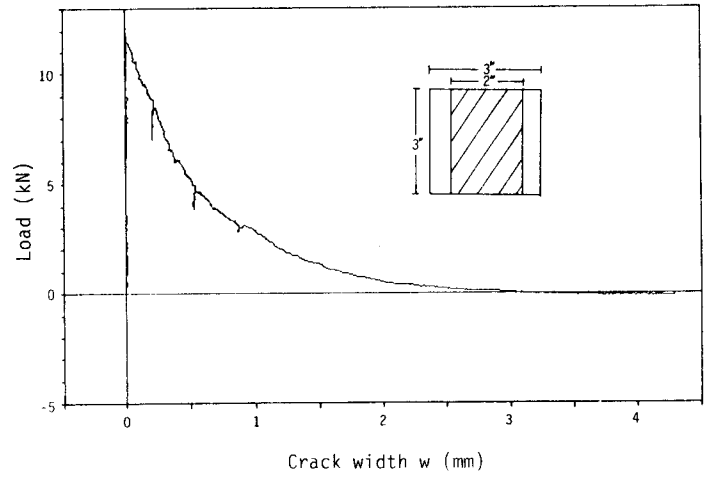

Figure 12. Result of a Stable Direct Tension Test on Mortar Reinforced with 2% LCP Fiber l=12.7mm, d=22.6 μm, Insert shows X-section of Specimen with Side Notches.

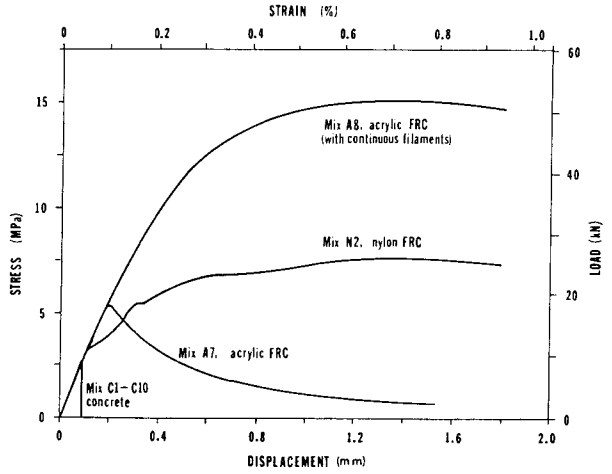

Figure 13. Improved Ductility in FRC Beams under Flexural Load [20]

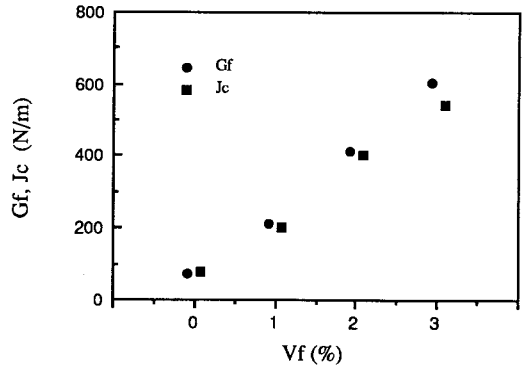

Figure 14. Fracture Toughness of Acrylic Fiber Reinforced Concrete [4]

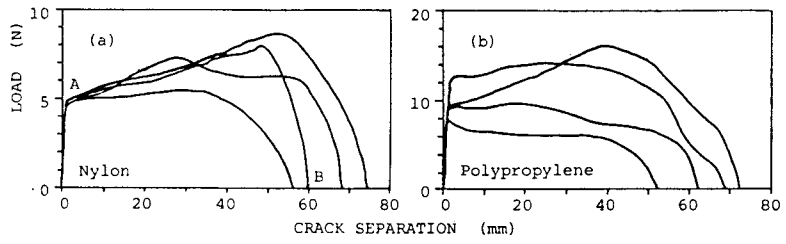

Figure 15. Load vs. Crack Separation Curves from Pull-out Tests [21]

Figure 16. SEM graph of Abraded Surface of a Nylon Fiber Subsequent to Pull-Out from a Cement Matrix

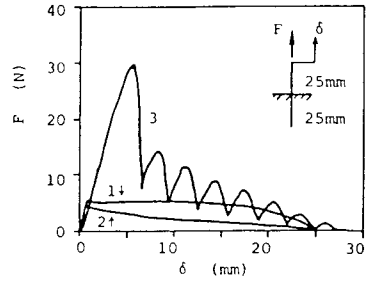

Figure 17. Pull-out Test of Nylon Fibers: 1-washed in hot water; 2-coated with fluorocarbon mold release; 3-crimped and coated with fluorocarbon mold release

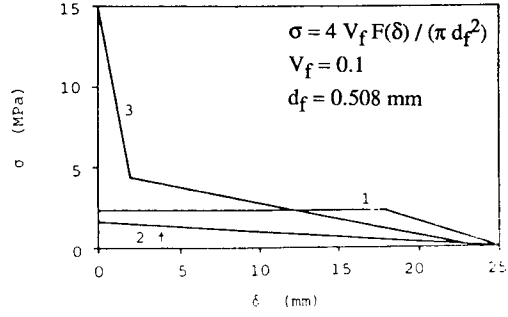

Figure 18. Approximate Tension-softening Curves from the Pull-out Test Results in Figure 17

To demonstrate the importance of fiber/matrix interfacial behavior on FRC toughness, pull-out test of nylon fiber reinforced mortar was conducted [22]. The test curves shown in Figure 17 are for the same fiber treated in three different manners. One fiber (1) was washed in hot water to remove the oil-based finish to increase fiber abrasion. One fiber (2) was coated with fluorocarbon mold release to reduce fiber abrasion. Another one (3) was crimped and subsequently coated with fluorocarbon mold release agent. Crimping was performed by running the fiber through a set of gears. The pull-out curve for a fiber with crimping only (not shown) leads to very high pull-out load and the fiber ruptures instead of sliding out.

The $\sigma-\delta$ curves for an ideal FRC with such fibers assuming that the fibers cross perpendicularly the crack plane may be estimated from the fiber volume fraction. This is shown in Figure 18 for the nylon fiber with these three different fiber treatments. The significant differences in the tension-softening behavior associated with differences in interfacial behavior may be expected to occur in FRC with random fiber orientation as well. The fracture toughness for the idealized FRC is illustrated in Figure 19.

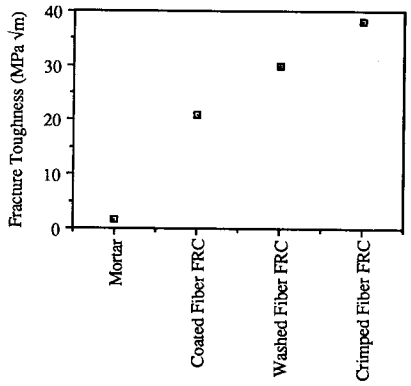

Figure 19. Effect of Fiber Treatment on Synthetic FRC Toughness

These studies show that the fracture toughness in FRC may be significantly enhanced by fiber damage during the pull-out process. Crimping provides a possible avenue of engineering toughness with synthetic fiber reinforced concrete. However, if bonding is too strong, or fiber aspect ratio too large, fiber fracture may occur instead of pull-out, leading to lower composite toughness.

CONCLUSIONS

The experimental study of toughening mechanisms in plain and fiber reinforced concrete, in combination with theoretical models relating material internal structures to composite properties, is very useful in systematic engineering of fracture toughness into these materials. They also provide guidelines in optimization of competing properties such as toughness versus strength. It is

demonstrated that the presence of weak interfaces in plain concrete and FRC is crucial to providing enhanced toughness. In plain concrete the weak interface is at the aggregate/cement interface; whereas in FRC the weak interface is at the fiber/cement interface. Toughness engineering may aim at increasing the amount of such weak interfaces through V_f or R_{max} of aggregates, and V_f of fibers. However such increases are limited by workability problems of the material in the fresh state. An alternative approach would be to engineer the interface to increase the inelastic energy dissipation at such interfaces.

In high strength concrete, reduction of weak interfaces (e.g. due to small R_{max} or elimination of weak interfacial zone) leads to low fracture toughness. Introduction of fibers and hence weak interface in this system may prevent excess brittleness, although it may be expected that certain amount of strength reduction would result. Work along this line is now in progress at the Center for Advanced Construction Materials at MIT.

ACKNOWLEDGEMENTS

Useful discussions with S. Backer, J. Huang and Y. Wang, and grant support from the Shimizu Corporation and the National Science Foundation, are gratefully acknowledged.

REFERENCES

1. J.R.Rice, J.of Applied Mechanics, 379 (1968).
2. A.J. Zielinski, Report 5-83-5, Stevin Lab., Delft U. of Techn. (1983).
3. A.Hillerborg, Report to RILEM, TC50-FMC, Lund Sweden, (1984).
4. R. Ward, K. Yamanobe, V.C. Li and S. Backer, in Application of Fracture Mechanics to Cementitous Materials and Structures, edited by V.C. Li and Z. Bazant, ACI, in press (1988).
5. V.C. Li and E. Liang, ASCE J. Eng. Mech., 112 (6), 566 (1986).
6. A.R. Ingraffea and W.H. Gerstle, in Application of Fracture Mechanics to Cementitous Composites, edited by S.P. Shah, Martinus Nijhoff, Dordrescht, 247 (1985).
7. Y.W. Mai, this volume (1988).
8. F.H. Wittmann, in Fracture Mechanics of Concrete, edited F.H. Wittmann, 43 (1983).
9. F.O.Slate and R.F.Matheus, J. Amer. Concr. Inst. Proc., 64, 1, 34 (1967).
10. F.O.Slate and K.O.Hover, in Fracture Mechanics of Concrete, edited by A.Carpinteri and A.R.Ingraffea, 137 (1984).
11. Yu.V.Zaitsev, in Mechanics of Geomaterials, edited by Z.Bazant, 109 (1985).
12. V.C. Li and J. Huang, International J. Engineering Frac. Mech., submitted (1988).
13. J. Huang and V.C. Li, in preparation (1988).
14. K.T.Faber, A.G.Evans and M.D.Drory, in Fracture Mechanics of Ceramics, 6, edited by R.C.Bradt et al., 77 (1983).
15. H.A.W. Cornelissen, D.A. Hordijk and H.W. Reinhardt, in Fracture Toughness and Fracture Energy of Concrete, edited by F.H. Wittmann, 565 (1986).
16. Mihashi, N. Nomura and F.H. Wittmann, this volume (1988).
17. S.P.Shah and F.J.McGarry, J. of Engineering Mechanics Division, Proc. ASCE, 1663 (1971).
18. J.L. Lott and C.E. Kesler, Report No. 648, Dept. of Theo. and Appl. Mech. U. Illinois at Urbana (1984).

19. A.B. Owen, Ph.D. Thesis, U. Cambridge (1979).
20. Y. Wang, S. Backer and V.C. Li, J. Mat. Sci., 22 4281 (1987).
21. Y. Wang, V.C. Li and S. Backer, in Bonding in Cementitious Materials, edited by S.Mindess and S.P. Shah, MRS 114, in press (1988).
22. V.C. Li, Y. Wang and S. Backer, in Bonding in Cementitious Materials, edited by S.Mindess and S.P. Shah, MRS 114, in press (1988).